Stochastic differential equation for a system coupled to a thermostatic bath via an arbitrary interaction Hamiltonian

Jong-Min Park,[1,2,3] Hyunggyu Park,[4] and Jae Sung Lee[3,*]
[1]*Asia Pacific Center for Theoretical Physics, Pohang 37673, Korea*
[2]*Department of Physics, Postech, Pohang 37673, Korea*
[3]*School of Physics, Korea Institute for Advanced Study, Seoul 02455, Korea*
[4]*Quantum Universe Center, Korea Institute for Advanced Study, Seoul 02455, Korea*

(Received 22 September 2023; revised 15 May 2024; accepted 20 June 2024; published 29 July 2024)

The conventional Langevin equation offers a mathematically convenient framework for investigating open stochastic systems interacting with their environment or a bath. However, it is not suitable for a wide variety of systems whose dynamics rely on the nature of the environmental interaction, as the equation does not incorporate any specific information regarding that interaction. Here, we present a stochastic differential equation (SDE) for an open system coupled to a thermostatic bath via an arbitrary interaction Hamiltonian. This SDE encodes the interaction information to a fictitious potential (mean force) and a position-dependent damping coefficient. Surprisingly, we find that the conventional Langevin equation can be recovered in the presence of arbitrary strong interactions given two conditions: translational invariance of the potential and mutual independence of baths. Our results provide a comprehensive framework for studying open stochastic systems with an arbitrary interaction Hamiltonian and yield deeper insight into why various experiments fit the conventional Langevin description regardless of the strength or type of interaction.

DOI: 10.1103/PhysRevE.110.014143

I. INTRODUCTION

An open system interacts with its environment or bath, and its dynamics depend on the nature of the system-bath (SB) interaction. Therefore, information on the full Hamiltonian, including the environment, is necessary to understand and describe the dynamics of an open system accurately. In most cases, however, the huge number of degrees of freedom for the environment renders this approach impractical. Thus, an effective and phenomenological equation of motion is required to describe the process of an open system approximately. In this context, a mesoscopic stochastic differential equation (SDE), such as the Langevin equation, has been widely used to successfully describe open systems with continuous time and space. This SDE, where simple dissipation and noise terms are used to represent the SB interaction effect, has enabled the derivation of important relations in stochastic thermodynamics, including fluctuation theorems [1–4], thermodynamic uncertainty relations [5–13], and speed limit [14–24].

Although the conventional SDE is successful, it fails to capture the specific nature of the SB interaction. This interaction can be neglected at the macroscopic scale, given that the SB interaction Hamiltonian is inversely proportional to the system size in comparison to the volume Hamiltonian unless the interaction is of long-range. However, at a small scale, the SB interaction Hamiltonian is comparable to the system Hamiltonian and thus cannot be neglected, as it will affect the dynamics of the system significantly [25,26]. Unfortunately, the specific nature of the SB interaction is not included in the conventional Langevin equation, limiting the ability to study small open systems that are strongly coupled to a bath [27,28]. As a result, the thermodynamics of small systems with strong SB interaction has not been investigated systematically.

In this paper, we develop an SDE to capture the nature of the SB interactions, which is applicable to a system coupled to a thermostatic bath via arbitrary SB interactions. Instead of solely considering the deterministic Hamiltonian dynamics of the system and bath, we introduce a *super bath* that enables the bath to be thermalized. This setup facilitates obtaining the desired SDE without relying on other assumptions used to ensure the equilibrium bath in previous approaches [29–33]. The proposed SDE encodes information regarding the SB interaction into two terms: the *mean-force* term, which is a fictitious conservative force applied to a system that modifies the equilibrium state from the ordinary Gibbs state of the system Hamiltonian, and a position-dependent damping tensor. Remarkably, we identify two physical conditions that can lead to the vanishing of SB interaction effects, even in the case of strong coupling. These conditions correspond to the *translational invariance* of the interaction potentials and the *mutual independence* of baths. Under these conditions, we demonstrate that our SDE reduces to the conventional Langevin equation without incorporating any information regarding the SB interaction specifics. This clearly shows that the conventional Langevin equation and the Gibbs state of the system Hamiltonian can be obtained as an equilibrium state without the assumption of a weak interaction.

*Contact author: jslee@kias.re.kr

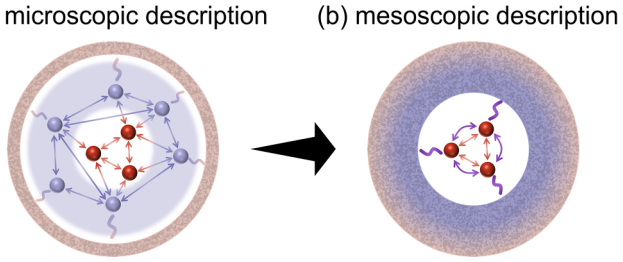

FIG. 1. Schematic illustration of the microscopic description (a) and the effective mesoscopic description (b). Red and blue balls denote the system and bath particles, respectively, and the outer reddish ring represents the thermostat connected to bath particles in (a). Wavy curves and arrows depict thermal contact to thermostat and the interactions between particles, respectively. In (b), the outer circular area with gradient colors and the wavy purple curves denote the effective bath and the thermal contact between system particles and the effective bath, respectively.

II. SDE FOR ARBITRARY SYSTEM-BATH INTERACTIONS

A. Microscopic setup

We begin by considering an SB composite, as illustrated in Fig. 1(a). The system and the bath consist of N and $\tilde{N}$ particles, each with mass m and $\tilde{m}$, respectively. The particles interact with each other via certain potentials. We will use the notation $\tilde{\square}$ for denoting quantities belonging to the bath. For brevity of presentation, we restrict our discussion to a one-dimensional space; however, extension to higher dimensional spaces is straightforward. The position and velocity of the nth system particle at time t are denoted as $x_n(t)$ and $v_n(t)$ for $n = 1, 2, ..., N$, respectively. Similarly, $\tilde{x}_{\tilde{n}}(t)$ and $\tilde{v}_{\tilde{n}}(t)$ for $\tilde{n} = 1, 2, ..., \tilde{N}$ denote the position and velocity of the $\tilde{n}$th bath particle at time t. For maintaining the bath temperature, the bath particles are connected to a Langevin thermostat with temperature T and damping constant $\tilde{\gamma}$. This is a typical setup for various molecular dynamics (MD) simulations. The microscopic equations of motion for the system and bath particles are given by

$$\begin{aligned} \text{system}: \ & \boldsymbol{v}(t) = \dot{\boldsymbol{x}}(t), \\ & m\dot{\boldsymbol{v}}(t) = \boldsymbol{f}(\boldsymbol{x}(t), \boldsymbol{v}(t), t) - \nabla_x V_{\mathrm{I}}(\boldsymbol{x}(t), \tilde{\boldsymbol{x}}(t)), \\ \text{bath}: \ & \tilde{\boldsymbol{v}}(t) = \dot{\tilde{\boldsymbol{x}}}(t), \\ & \tilde{m}\dot{\tilde{\boldsymbol{v}}}(t) = -\nabla_{\tilde{x}} V_{\mathrm{I}}(\boldsymbol{x}(t), \tilde{\boldsymbol{x}}(t)) - \tilde{\gamma}\tilde{\boldsymbol{v}}(t) + \tilde{\boldsymbol{\xi}}(t), \end{aligned} \tag{1}$$

where $\boldsymbol{x} = (x_1, \cdots, x_N)^{\mathsf{T}}$, $\boldsymbol{v} = (v_1, \cdots, v_N)^{\mathsf{T}}$, $\tilde{\boldsymbol{x}} = (\tilde{x}_1, \cdots, \tilde{x}_{\tilde{N}})^{\mathsf{T}}$, $\tilde{\boldsymbol{v}} = (\tilde{v}_1, \cdots, \tilde{v}_{\tilde{N}})^{\mathsf{T}}$, $\nabla_x = (\partial_{x_1}, \cdots, \partial_{x_N})^{\mathsf{T}}$, and $\nabla_{\tilde{x}} = (\partial_{\tilde{x}_1}, \cdots, \partial_{\tilde{x}_{\tilde{N}}})^{\mathsf{T}}$, with T denoting the matrix transpose. $\boldsymbol{f}(\boldsymbol{x}, \boldsymbol{v}, t)$ represents a force acting on the system particles and $V_{\mathrm{I}}(\boldsymbol{x}, \tilde{\boldsymbol{x}}) = H_{\mathrm{I}}(\boldsymbol{x}, \tilde{\boldsymbol{x}}) + \tilde{\Phi}(\tilde{\boldsymbol{x}})$ is associated with the interaction potential, where $H_{\mathrm{I}}(\boldsymbol{x}, \tilde{\boldsymbol{x}})$ is the SB interaction Hamiltonian and $\tilde{\Phi}(\tilde{\boldsymbol{x}})$ is the potential exerted only on the bath particles. $\tilde{\boldsymbol{\xi}} = (\tilde{\xi}_1, \cdots, \tilde{\xi}_{\tilde{N}})^{\mathsf{T}}$ is the Gaussian white noise with zero mean and $\langle \tilde{\xi}_i(t)\tilde{\xi}_j(t')\rangle = 2\tilde{\gamma}T\delta_{ij}\delta(t-t')$ in Boltzmann constant units ($k_{\mathrm{B}} = 1$). Note that the thermostat connected to the bath has been referred to as a *superbath* in the literature [1,25,26].

Equilibrium of the total system (system and bath) is achievable when a conservative force is solely applied to the system, that is, $\boldsymbol{f}(\boldsymbol{x}, \boldsymbol{v}, t) = -\nabla_x \Phi(\boldsymbol{x})$. Then, the equilibrium distribution p^{eq} of the total system is simply given by the Gibbs state as

$$p^{\mathrm{eq}}(\boldsymbol{x}, \boldsymbol{v}, \tilde{\boldsymbol{x}}, \tilde{\boldsymbol{v}}) \equiv \frac{1}{\mathcal{Z}} e^{-\beta(H(\boldsymbol{x},\boldsymbol{v}) + H_{\mathrm{I}}(\boldsymbol{x},\tilde{\boldsymbol{x}}) + \tilde{H}(\tilde{\boldsymbol{x}},\tilde{\boldsymbol{v}}))}, \tag{2}$$

where $H(\boldsymbol{x}, \boldsymbol{v}) = m\boldsymbol{v}^{\mathsf{T}}\boldsymbol{v}/2 + \Phi(\boldsymbol{x})$ is the system Hamiltonian, $\tilde{H}(\tilde{\boldsymbol{x}}, \tilde{\boldsymbol{v}}) = \tilde{m}\tilde{\boldsymbol{v}}^{\mathsf{T}}\tilde{\boldsymbol{v}}/2 + \tilde{\Phi}(\tilde{\boldsymbol{x}})$ is the bath Hamiltonian, $\mathcal{Z}$ is the partition function for the total Hamiltonian $H + H_{\mathrm{I}} + \tilde{H}$, and $\beta = 1/T$ is the inverse temperature. Integrating out Eq. (2) over the bath variables yields the equilibrium distribution for the system as follows:

$$\begin{aligned} p^{\mathrm{eq}}_{\mathrm{sys}}(\boldsymbol{x}, \boldsymbol{v}) &\equiv \int d\tilde{\boldsymbol{x}} d\tilde{\boldsymbol{v}}\, p^{\mathrm{eq}}(\boldsymbol{x}, \boldsymbol{v}, \tilde{\boldsymbol{x}}, \tilde{\boldsymbol{v}}) \\ &= \frac{1}{\mathcal{Z}_{\mathrm{sys}}} e^{-\beta(H(\boldsymbol{x},\boldsymbol{v}) + \Delta(\boldsymbol{x}))}, \end{aligned} \tag{3}$$

where $\mathcal{Z}_{\mathrm{sys}}$ is the partition function for the Hamiltonian $H + \Delta$ and $\Delta(\boldsymbol{x})$ is a fictitious potential known as the potential of the mean force [27], defined as

$$\Delta(\boldsymbol{x}) \equiv -T \ln \frac{\mathcal{Z}_{\mathrm{I}}(\boldsymbol{x})}{\mathcal{Z}_{\tilde{\Phi}}} \tag{4}$$

with $\mathcal{Z}_{\mathrm{I}} = \int d\tilde{\boldsymbol{x}} e^{-\beta V_I(\boldsymbol{x},\tilde{\boldsymbol{x}})}$ and $\mathcal{Z}_{\tilde{\Phi}} = \int d\tilde{\boldsymbol{x}} e^{-\beta\tilde{\Phi}(\tilde{\boldsymbol{x}})}$. The distribution $p^{\mathrm{eq}}_{\mathrm{sys}}$ in Eq. (3) is certainly different from the Gibbs state of the system Hamiltonian $p^{\mathrm{G}}_{\mathrm{sys}} \equiv e^{-\beta H}/\mathcal{Z}^{\mathrm{G}}_{\mathrm{sys}}$ with $\mathcal{Z}^{\mathrm{G}}_{\mathrm{sys}} = \int d\boldsymbol{x} d\boldsymbol{v} e^{-\beta H(\boldsymbol{x},\boldsymbol{v})}$, unless $\Delta = 0$. Since vanishing of Δ is achieved for negligible H_{I}, it is generally accepted that the weak interaction (small H_{I}) limit is necessary for an equilibrium distribution of a system being $p^{\mathrm{G}}_{\mathrm{sys}}$. However, since the weak interaction limit amounts to isolating the system from the environment, heat transfer or relaxation is unlikely to occur under these conditions [34,35]. This contradicts the usual Langevin-system experiments, in which relaxation takes place quickly and the equilibrium state is given by $p^{\mathrm{G}}_{\mathrm{sys}}$. This strongly suggests that there exists another mechanism that leads to Δ vanishing rather than the weak interaction.

B. Brief sketch of mesoscopic SDE derivation

The derivation of the mesoscopic SDE for a system is based on timescale separation, in which the variables of the bath are treated as fast variables compared to those of the system. The derivation procedure can be divided into two steps. The first step is taking the overdamped limit of the equation of motion for the bath, which is mathematically equivalent to the limit of small $\tilde{m}/\tilde{\gamma}$. The second step is called *adiabatic elimination* [36], where the bath variables are integrated out in the small $\tilde{\gamma}$ limit. The details are presented in Sec. IV. After integrating out all bath variables via this procedure, the resulting mesoscopic SDE is

$$m\dot{\boldsymbol{v}} = \boldsymbol{f}(\boldsymbol{x}, \boldsymbol{v}, t) - \nabla_x \Delta(\boldsymbol{x}) - \mathsf{G}(\boldsymbol{x}) \cdot \boldsymbol{v} + \boldsymbol{\xi}, \tag{5}$$

where the Gaussian white noise $\boldsymbol{\xi} = (\xi_1, \cdots, \xi_N)^{\mathsf{T}}$ is characterized by $\langle \boldsymbol{\xi}(t)\boldsymbol{\xi}^{\mathsf{T}}(t')\rangle = 2T\mathsf{G}(\boldsymbol{x}(t))\delta(t-t')$ with zero mean. Here, $\mathsf{G}(\boldsymbol{x})$ is the effective damping tensor whose (n, m) element is given by

$$\mathsf{G}_{n,m}(\boldsymbol{x}) = \frac{1}{T}\int_0^\infty dt\, C_{\partial_{x_n} V_{\mathrm{I}}, \partial_{x_m} V_{\mathrm{I}}}(t|\boldsymbol{x}), \tag{6}$$

with the correlation $C_{h,g}(t|\boldsymbol{x})$ of two arbitrary functions $h(\boldsymbol{x},\tilde{\boldsymbol{x}})$ and $g(\boldsymbol{x},\tilde{\boldsymbol{x}})$ in the equilibrium dynamics of bath variables $\tilde{\boldsymbol{x}}(t)$ at a fixed system state $\boldsymbol{x}$. By denoting the average over the equilibrium sample paths of the bath at a given $\boldsymbol{x}$ by $\langle\Box\rangle_{\rm b}^{\rm eq}$, the correlation can be expressed as

$$C_{h,g}(t|\boldsymbol{x}) \equiv \langle \delta h(\boldsymbol{x},\tilde{\boldsymbol{x}}(t))\delta g(\boldsymbol{x},\tilde{\boldsymbol{x}}(0))\rangle_{\rm b}^{\rm eq}, \tag{7}$$

where $\delta h(\boldsymbol{x},\tilde{\boldsymbol{x}}) = h(\boldsymbol{x},\tilde{\boldsymbol{x}}) - \langle h(\boldsymbol{x},\tilde{\boldsymbol{x}})\rangle_{\rm b}^{\rm eq}$ represents the deviation of a function $h(\boldsymbol{x},\tilde{\boldsymbol{x}})$. Note that the damping tensor $\mathsf{G}(\boldsymbol{x})$ in Eq. (6) depends on the specific form of the SB interaction $H_{\rm I}(\boldsymbol{x},\tilde{\boldsymbol{x}})$. In addition, the symmetry $C_{f,g}(t|\boldsymbol{x}) = C_{g,f}(t|\boldsymbol{x})$ is ensured by the microreversibility $C_{f,g}(t|\boldsymbol{x}) = C_{f,g}(-t|\boldsymbol{x})$ and time homogeneity of the bath's equilibrium dynamics at a fixed $\boldsymbol{x}$.

The SDE (5) includes two terms reflecting the strong coupling effects: (i) the potential of the mean force Δ and (ii) the effective damping tensor G. Since the fluctuation-dissipation relation holds, G has no effect on the equilibrium state, but only affects the relaxation dynamics. On the other hand, Δ modifies the equilibrium distribution in accordance with Eq. (3). Thus, this SDE provides a comprehensive mesoscopic description, as illustrated in Fig. 1(b), for studying dynamics, as well as the steady states of open stochastic systems with arbitrary interaction Hamiltonians.

III. CONDITIONS FOR VANISHING OF INTERACTION SPECIFICS

We identify two physical conditions that are essential for eliminating the effects of the interaction specifics and restoring Eq. (5) to the conventional Langevin equation. To simplify the explanation, we initially focus on the case of a single-particle system ($N = 1$). In this case, SB coupling effects vanish when the *translational invariance* of the interaction potential $V_{\rm I}(x_1,\tilde{\boldsymbol{x}})$ is satisfied. Here, translational invariance means $V_{\rm I}(x_1,\tilde{\boldsymbol{x}}) = V_{\rm I}(x_1+a,\tilde{\boldsymbol{x}}+\tilde{\boldsymbol{a}})$, where a is an arbitrary constant and $\tilde{\boldsymbol{a}}$ is the $\tilde{N}$-dimensional vector with all elements being equal to a in one spatial dimension. In other words, the interaction potential is not altered by an arbitrary translational shift, as illustrated in Fig. 2(a). The condition of translational invariance is usually valid for experiments implemented in the bulk region (far from the boundary) of their environment.

Under the condition of translational invariance, by taking $a = -x_1$, one can write

$$V_{\rm I}(x_1,\tilde{\boldsymbol{x}}) = V_{\rm I}(0,\tilde{\boldsymbol{X}}), \tag{8}$$

where $\tilde{X}_{\tilde{n}} \equiv \tilde{x}_{\tilde{n}} - x_1$. Accordingly, the potential of the mean force (4) can be expressed as

$$\Delta = -T\ln\int d\tilde{\boldsymbol{X}}\, e^{-\beta V_{\rm I}(0,\tilde{X})} + T\ln\mathcal{Z}_{\tilde{\Phi}}, \tag{9}$$

where $\int d\tilde{\boldsymbol{X}}$ indicates integration over all $\tilde{X}_{\tilde{n}}$ variables. Since the integrand in Eq. (9) is a function of only $\tilde{X}_{\tilde{n}}$, Δ has no dependence on the position of the system particle. Consequently, the mean force term $\nabla_x\Delta$ in Eq. (5) vanishes.

We can also demonstrate that translational invariance results in the removal of the dependence of the damping tensor on the SB interaction potential. When translational invariance holds, the interaction potential $V_{\rm I}$ becomes a function of the position differences between all pairs of particles, as detailed

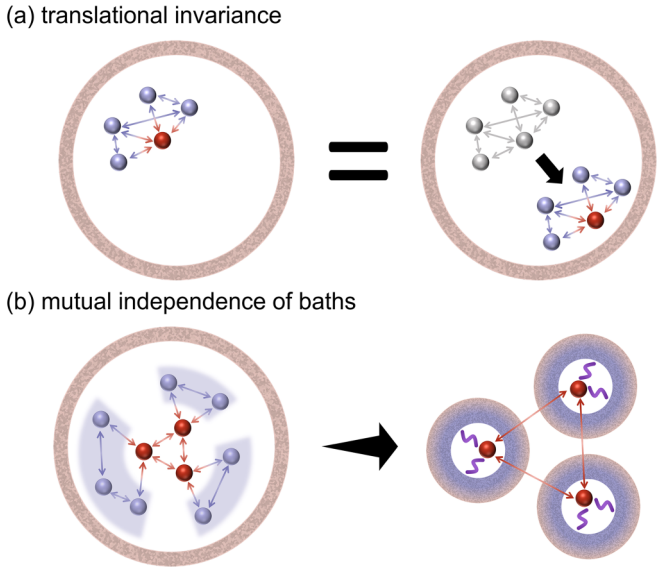

FIG. 2. Schematic diagram of the two conditions for vanishing of interaction specifics. (a) Translational invariance. This is the condition that interaction potentials for any pairs of particles are invariant under an arbitrary translational shift. (b) Mutual independence of baths. This condition disallows that each bath particle interacts with multiple system particles simultaneously. Thus, all bath particles can be disjointly partitioned into subgroups interacting with respective system particles. Interactions between bath particles belonging to other groups are prohibited.

in the Supplemental Material (SM) [37]. Then, the action-reaction law leads to

$$-\partial_{x_1}V_{\rm I}(x_1,\tilde{\boldsymbol{x}}) - \sum_{\tilde{n}}\partial_{\tilde{x}_{\tilde{n}}}V_{\rm I}(x_1,\tilde{\boldsymbol{x}}) = 0. \tag{10}$$

Using Eq. (10), we can rewrite Eq. (6) as

$$\mathsf{G}_{1,1} = \frac{1}{T}\sum_{\tilde{n},\tilde{m}}\int_0^\infty dt\, C_{\partial_{\tilde{x}_{\tilde{n}}}V_{\rm I},\partial_{\tilde{x}_{\tilde{m}}}V_{\rm I}}(t|x_1). \tag{11}$$

The correlation C in Eq. (11) is written in terms of the force applied to the bath particles. Hence, Eq. (11) differs from the original definition in Eq. (6), which is expressed by the force exerted on the system particles. Now, one can utilize the generalized Green-Kubo relation [38] written as

$$\int_0^\infty dt C_{\partial_{\tilde{x}_{\tilde{n}}}V_{\rm I},\partial_{\tilde{x}_{\tilde{m}}}V_{\rm I}}(t|x_1) = \tilde{\gamma}T\delta_{\tilde{n},\tilde{m}}. \tag{12}$$

The derivation of this relation is presented in the SM [37]. By applying the generalized Green-Kubo relation to Eq. (11), we arrive at

$$\mathsf{G}_{1,1} = \gamma_1 \equiv \tilde{N}\tilde{\gamma}. \tag{13}$$

No dependence on the SB interaction potential and system position remains in the damping tensor. Consequently, for a single-particle system, translational invariance of $V_{\rm I}$ is the unique condition for the vanishing of the SB-coupling effects.

For multparticle systems, however, the SB coupling effects can remain even when the translational invariance of $V_{\rm I}$ holds. This can be easily understood from the following

example. If we consider a two-particle system, the interaction potential satisfies $V_{\rm I}(x_1, x_2, \tilde{\boldsymbol{x}}) = V_{\rm I}(0, x_2 - x_1, \tilde{\boldsymbol{X}})$, where $\tilde{X}_{\tilde{n}} \equiv \tilde{x}_{\tilde{n}} - x_1$. Then, the potential of the mean force is given by

$$\Delta = -T \ln \int d\tilde{\boldsymbol{X}}\, e^{-\beta V_{\rm I}(0, x_2 - x_1, \tilde{\boldsymbol{X}})} + T \ln \mathcal{Z}_{\tilde{\Phi}}.$$

Thus, Δ depends on the positions of the system and, as a result, the term $\boldsymbol{\nabla}_x \Delta$ does not vanish. In addition, since the action-reaction law for a multiparticle system is written as $-\sum_n \partial_{x_n} V_{\rm I}(x_1, \tilde{\boldsymbol{x}}) - \sum_{\tilde{n}} \partial_{\tilde{x}_{\tilde{n}}} V_{\rm I}(x_1, \tilde{\boldsymbol{x}}) = 0$, the correlation C cannot be expressed solely in terms of the force applied to bath particles. Consequently, the damping tensor no longer takes the simple form as given in Eq. (13).

To eliminate the SB coupling effect for N-particle systems, we require an additional condition: *mutual independence* of baths. As illustrated in Fig. 2(b), this condition implies that the entire bath can be partitioned into N mutually independent subbaths, with each subbath exclusively interacting with one of the system particles. Thus, it prohibits each bath particle from interacting with multiple (more than one) system particles simultaneously. In other words, this condition amounts to the situation where each system particle is connected to its own subbath, and there are no interactions between subbaths. While achieving strict mutual independence of baths for multiparticle systems in typical experimental setups is nearly impossible, it can be approximately valid when the system particles are significantly farther apart from each other than the SB interaction range. We numerically verify this validity in Sec. V C.

Mutual Independence of baths can be mathematically expressed as $V_{\rm I}(\boldsymbol{x}, \tilde{\boldsymbol{x}}) = \sum_n V_n(x_n, \tilde{\boldsymbol{x}}_n)$, where $\tilde{\boldsymbol{x}}_n = (\tilde{x}_1, \cdots, \tilde{x}_{\tilde{N}_n})$ represents the positions of bath particles belonging to the nth subbath, which interact with the nth system particle. The parameter $\tilde{N}_n$ denotes the number of bath particles in the nth subbath. Thus, interactions occur exclusively among the system and bath particles with the same index n. Along with the translational invariance of $V_n(x_n, \tilde{\boldsymbol{x}}_n)$, the mutual independence enables us to decompose the interaction potential $V_{\rm I}$ as

$$V_{\rm I}(\boldsymbol{x}, \tilde{\boldsymbol{x}}) = \sum_n V_n(0, \tilde{\boldsymbol{X}}_n), \tag{14}$$

where $\tilde{\boldsymbol{X}}_n = (\tilde{x}_1 - x_n, \cdots, \tilde{x}_{\tilde{N}_n} - x_n)$. Then, the potential of the mean force can be calculated as

$$\Delta = -T \sum_n \ln \int d\tilde{\boldsymbol{X}}_n\, e^{-\beta V_n(\boldsymbol{0}, \tilde{\boldsymbol{X}}_n)} + T \ln \mathcal{Z}_{\tilde{\Phi}}. \tag{15}$$

As a consequence, Δ is independent of the positions of the system particles and the mean-force term $\boldsymbol{\nabla}_x \Delta$ in Eq. (5) vanishes. Furthermore, due to the separability of $V_{\rm I}(\boldsymbol{x}, \tilde{\boldsymbol{x}})$ into $V_n(x_n, \tilde{\boldsymbol{x}}_n)$, we can express the action-reaction law for each nth system particle as

$$-\partial_{x_n} V_n(x_n, \tilde{\boldsymbol{x}}_n) - \sum_{\tilde{n}_n=1}^{\tilde{N}_n} \partial_{\tilde{x}_{\tilde{n}_n}} V_n(x_n, \tilde{\boldsymbol{x}}_n) = 0. \tag{16}$$

Therefore, the (n, m) element of the damping tensor can be written in terms of only the force applied to the bath particles as

$$\mathsf{G}_{n,m} = \frac{1}{T} \sum_{\tilde{n}_n=1}^{\tilde{N}_n} \sum_{\tilde{n}_m=1}^{\tilde{N}_m} \int_0^\infty dt\, C_{\partial_{\tilde{x}_{\tilde{n}_n}} V_n, \partial_{\tilde{x}_{\tilde{n}_m}} V_m}(t|x_1). \tag{17}$$

From the generalized Green-Kubo relations, we finally arrive at

$$\mathsf{G}_{n,m} = \gamma_n \delta_{n,m} \quad (\gamma_n \equiv \tilde{N}_n \tilde{\gamma}). \tag{18}$$

As a result, the dependence of the damping tensor on the SB interaction potential and system positions disappears and only its diagonal elements survive.

Therefore, for even multiparticle systems, under the two conditions of translational invariance of $V_{\rm I}$ and mutual independence of baths, Eq. (5) simplifies to the conventional Langevin equation as follows:

$$m\dot{v}_n(t) = f_n(\boldsymbol{x}(t), \boldsymbol{v}(t), t) - \gamma_n v_n(t) + \xi_n(t), \tag{19}$$

where the noise correlation is given by $\langle \xi_n(t) \xi_m(t') \rangle = 2\gamma_n T \delta_{nm} \delta(t - t')$. This clearly shows that the conventional Langevin equation can be valid even in the presence of strong coupling under these two conditions.

IV. DERIVATION OF MESOSCOPIC SDE

The derivation of Eq. (5) is based on a proper timescale separation, where the bath variables are treated as fast variables, and thus integrated out under certain conditions. The derivation procedure can be divided into two steps. In the first step, the velocity variables of the bath are integrated out in the limit of small $\tilde{m}/\tilde{\gamma}$, which corresponds to the usual overdamped limit. Then, the corresponding Fokker-Plank equation reads

$$\dot{P}(\boldsymbol{x}, \boldsymbol{v}, \tilde{\boldsymbol{x}}, t) = \left(\mathcal{L} + \frac{1}{\tilde{\gamma}} \tilde{\mathcal{L}}_{\rm o} \right) P(\boldsymbol{x}, \boldsymbol{v}, \tilde{\boldsymbol{x}}, t), \tag{20}$$

where $P(\boldsymbol{x}, \boldsymbol{v}, \tilde{\boldsymbol{x}}, t)$ is the probability distribution function for the whole system and the Fokker-Planck operators with respect to the system and the (overdamped) bath are given by

$$\begin{aligned} \mathcal{L} &= -\boldsymbol{\nabla}_x^{\mathsf{T}} \boldsymbol{v} - \frac{1}{m} \boldsymbol{\nabla}_v^{\mathsf{T}} [\boldsymbol{f}(\boldsymbol{x}, \boldsymbol{v}, t) - \{\boldsymbol{\nabla}_x V_{\rm I}(\boldsymbol{x}, \tilde{\boldsymbol{x}})\}], \\ \tilde{\mathcal{L}}_{\rm o} &= \boldsymbol{\nabla}_{\tilde{x}}^{\mathsf{T}} [\{\boldsymbol{\nabla}_{\tilde{x}} V_{\rm I}(\boldsymbol{x}, \tilde{\boldsymbol{x}})\} + T \boldsymbol{\nabla}_{\tilde{x}}], \end{aligned} \tag{21}$$

respectively, where $\boldsymbol{\nabla}_v = (\partial_{v_1}, \cdots, \partial_{v_N})^{\mathsf{T}}$. The curly bracket $\{\square\}$ in Eq. (21) is used to indicate that derivative operators inside the bracket have no effect on terms outside of it. The overall factor $\tilde{\gamma}^{-1}$ in front of $\tilde{\mathcal{L}}_{\rm o}$ in Eq. (20) indicates that the relaxation timescale of the bath is proportional to the damping constant. Thus, the time separation can be implemented by taking the limit of small $\tilde{\gamma}$. This method is known as adiabatic elimination [36]. We note that to simultaneously satisfy these two limits, the small $\tilde{m}/\tilde{\gamma}$ limit and the small $\tilde{\gamma}$ limit, in numerical calculations, we have to choose a value of $\tilde{\gamma}$ that is small enough to ensure the bath particle remains in the equilibrium state, yet much larger compared to the mass of the bath particles. For completeness, we present the detailed procedure in the following.

We first consider the eigenfunctions $\varphi_k(\tilde{\boldsymbol{x}}|\boldsymbol{x})$ of $\tilde{\mathcal{L}}_\mathrm{o}$ and corresponding eigenvalues $-\lambda_k$ for a given $\boldsymbol{x}$, that is,

$$\tilde{\mathcal{L}}_\mathrm{o}\varphi_k(\tilde{\boldsymbol{x}}|\boldsymbol{x}) = -\lambda_k\varphi_k(\tilde{\boldsymbol{x}}|\boldsymbol{x}). \tag{22}$$

Note that in our sign convention, λ_k is always positive except for $\lambda_0 = 0$ which is the eigenvalue of the stationary-state distribution $\varphi_0(\tilde{\boldsymbol{x}}|\boldsymbol{x})$ of $\tilde{\mathcal{L}}_\mathrm{o}$ given by

$$\varphi_0(\tilde{\boldsymbol{x}}|\boldsymbol{x}) = \frac{1}{\mathcal{Z}_\mathrm{I}(\boldsymbol{x})}e^{-\beta V_\mathrm{I}(\boldsymbol{x},\tilde{\boldsymbol{x}})}, \tag{23}$$

with the partition function $\mathcal{Z}_\mathrm{I}(\boldsymbol{x}) = \int d\tilde{\boldsymbol{x}}e^{-\beta V_\mathrm{I}(\boldsymbol{x},\tilde{\boldsymbol{x}})}$. Thus, $\varphi_0(\tilde{\boldsymbol{x}}|\boldsymbol{x})$ is an equilibrium distribution of the overdamped bath for a given $\boldsymbol{x}$.

Now we expand the probability distribution function in terms of $\varphi_k(\tilde{\boldsymbol{x}}|\boldsymbol{x})$ as

$$P(\boldsymbol{x}, \boldsymbol{v}, \tilde{\boldsymbol{x}}, t) = \sum_k C_k(\boldsymbol{x}, \boldsymbol{v}, t)\varphi_k(\tilde{\boldsymbol{x}}|\boldsymbol{x}). \tag{24}$$

We define $\varphi_k^\dagger(\tilde{\boldsymbol{x}}|\boldsymbol{x})$ as an eigenfunction of the adjoint operator $\tilde{\mathcal{L}}_\mathrm{o}^\dagger$. Then it satisfies the eigenvalue equation $\tilde{\mathcal{L}}^\dagger\varphi_k^\dagger(\tilde{\boldsymbol{x}}|\boldsymbol{x}) = -\lambda_k\varphi_k^\dagger(\tilde{\boldsymbol{x}}|\boldsymbol{x})$ and the orthogonality $\int d\tilde{\boldsymbol{x}}\varphi_k^\dagger(\tilde{\boldsymbol{x}}|\boldsymbol{x})\varphi_m(\tilde{\boldsymbol{x}}|\boldsymbol{x}) = \delta_{k,m}$. By multiplying $\varphi_k^\dagger(\tilde{\boldsymbol{x}}|\boldsymbol{x})$ to both sides of Eq. (24), integrating over $\tilde{\boldsymbol{x}}$, and using the orthogonality, we arrive at the following equation for the coefficient $C_k(\boldsymbol{x}, \boldsymbol{v}, t)$ as

$$\dot{C}_k(\boldsymbol{x}, \boldsymbol{v}, t) = \sum_{m\geqslant 0}\mathcal{F}_{k,m}C_m(\boldsymbol{x}, \boldsymbol{v}, t) - \frac{\lambda_k}{\tilde{\gamma}}C_k(\boldsymbol{x}, \boldsymbol{v}, t), \tag{25}$$

where the tilted-system-Fokker-Planck operator $\mathcal{F}_{k,m}$ is defined as

$$\mathcal{F}_{k,m} \equiv \int d\tilde{\boldsymbol{x}}\varphi_k^\dagger(\tilde{\boldsymbol{x}}|\boldsymbol{x})\mathcal{L}\varphi_m(\tilde{\boldsymbol{x}}|\boldsymbol{x}). \tag{26}$$

In the small $\tilde{\gamma}$ limit, one can write Eq. (25) up to the linear order in $\tilde{\gamma}$ as

$$\begin{aligned}\dot{C}_0(\boldsymbol{x}, \boldsymbol{v}, t) &= \sum_{m\geqslant 0}\mathcal{F}_{0,m}C_m(\boldsymbol{x}, \boldsymbol{v}, t) \quad \text{for } k = 0,\\ C_k(\boldsymbol{x}, \boldsymbol{v}, t) &= \frac{\tilde{\gamma}}{\lambda_k}\mathcal{F}_{k,0}C_0(\boldsymbol{x}, \boldsymbol{v}, t) + \mathcal{O}(\tilde{\gamma}^2) \quad \text{for } k \geqslant 1.\end{aligned} \tag{27}$$

By inserting the expression for C_k into the equation for C_0 in Eq. (27), we obtain the uncoupled equation of motion for C_0 as follows:

$$\dot{C}_0(\boldsymbol{x}, \boldsymbol{v}, t) = \mathcal{L}_\mathrm{r}C_0(\boldsymbol{x}, \boldsymbol{v}, t) + \mathcal{O}(\tilde{\gamma}^2), \tag{28}$$

where the reduced-system operator $\mathcal{L}_\mathrm{r}$ is

$$\mathcal{L}_\mathrm{r} \equiv \mathcal{F}_{0,0} + \tilde{\gamma}\sum_{k\geqslant 1}\frac{\mathcal{F}_{0,k}\mathcal{F}_{k,0}}{\lambda_k}. \tag{29}$$

Using $\varphi_0^\dagger(\tilde{\boldsymbol{x}}|\boldsymbol{x}) = 1$, we can show that C_0 is the marginal distribution of $P(\boldsymbol{x}, \boldsymbol{v}, \tilde{\boldsymbol{x}}, t)$ as

$$C_0(\boldsymbol{x}, \boldsymbol{v}, t) = \int d\tilde{\boldsymbol{x}}\varphi_0^\dagger(\tilde{\boldsymbol{x}}|\boldsymbol{x})P(\boldsymbol{x}, \boldsymbol{v}, \tilde{\boldsymbol{x}}, t) = P(\boldsymbol{x}, \boldsymbol{v}, t). \tag{30}$$

Thus, Eq. (28) is the Fokker-Planck equation for the reduced system.

The explicit form of $\mathcal{L}_\mathrm{r}$ can be obtained from the definition of the tilted operators in Eq. (26). By using the orthogonality of the eigenfunctions and the mean-force relation $\nabla_x\Delta(\boldsymbol{x}) = \int d\tilde{\boldsymbol{x}}\{\nabla_x V_\mathrm{I}(\boldsymbol{x}, \tilde{\boldsymbol{x}})\}\varphi_0(\tilde{\boldsymbol{x}}|\boldsymbol{x})$ from Eq. (4), one can show that

$$\mathcal{F}_{0,0} = -\nabla_x^\mathsf{T}\boldsymbol{v} - \frac{1}{m}\nabla_v^\mathsf{T}[\boldsymbol{f}(\boldsymbol{x}, \boldsymbol{v}, t) - \{\nabla_x\Delta(\boldsymbol{x})\}]. \tag{31}$$

Therefore, $\mathcal{F}_{0,0}$ corresponds to the deterministic evolution part of the reduced equation of motion in Eq. (5). Using the eigenfunction orthogonality and $\varphi_0^\dagger(\tilde{\boldsymbol{x}}|\boldsymbol{x}) = 1$, it is straightforward to show that

$$\mathcal{F}_{0,k} = \frac{1}{m}\nabla_v^\mathsf{T}\boldsymbol{b}_k, \tag{32}$$

with $\boldsymbol{b}_k \equiv \int d\tilde{\boldsymbol{x}}\{\nabla_x V_\mathrm{I}(\boldsymbol{x}, \tilde{\boldsymbol{x}})\}\varphi_k(\tilde{\boldsymbol{x}}|\boldsymbol{x})$. Similarly, we can also show that

$$\mathcal{F}_{k,0} = \left(\frac{1}{T}\boldsymbol{v} + \frac{1}{m}\nabla_v\right)^\mathsf{T}\boldsymbol{b}_k. \tag{33}$$

For deriving Eq. (33), the relations $\nabla_x^\mathsf{T}\boldsymbol{v}\varphi_0(\tilde{\boldsymbol{x}}|\boldsymbol{x}) = \boldsymbol{v}^\mathsf{T}\{\nabla_x\varphi_0(\tilde{\boldsymbol{x}}|\boldsymbol{x})\} + \boldsymbol{v}^\mathsf{T}\varphi_0(\tilde{\boldsymbol{x}}|\boldsymbol{x})\nabla_x$, $\nabla_x\varphi_0(\tilde{\boldsymbol{x}}|\boldsymbol{x}) = -\beta\{\nabla_x V_\mathrm{I}\}\varphi_0(\tilde{\boldsymbol{x}}|\boldsymbol{x}) - \{\nabla_x \ln\mathcal{Z}_\mathrm{I}\}\varphi_0(\tilde{\boldsymbol{x}}|\boldsymbol{x})$, and $\varphi_k(\tilde{\boldsymbol{x}}|\boldsymbol{x}) = \varphi_k^\dagger(\tilde{\boldsymbol{x}}|\boldsymbol{x})\varphi_0(\tilde{\boldsymbol{x}}|\boldsymbol{x})$ are used in order. Plugging Eqs. (31)–(33) into Eq. (29) yields

$$\begin{aligned}\mathcal{L}_\mathrm{r} = &-\nabla_x^\mathsf{T}\boldsymbol{v} - \frac{1}{m}\nabla_v^\mathsf{T}[\boldsymbol{f}(\boldsymbol{x}, \boldsymbol{v}, t) - \{\nabla_x\Delta(\boldsymbol{x})\}]\\ &+ \frac{1}{m}\nabla_v^\mathsf{T}\mathsf{G}(\boldsymbol{x})\left(\boldsymbol{v} + \frac{T}{m}\nabla_v\right),\end{aligned} \tag{34}$$

with the damping tensor

$$\mathsf{G}(\boldsymbol{x}) \equiv \frac{\tilde{\gamma}}{T}\sum_{k\geqslant 1}\frac{\boldsymbol{b}_k\boldsymbol{b}_k^\mathsf{T}}{\lambda_k}. \tag{35}$$

This form clearly shows that the damping tensor is symmetric.

The remaining task is showing that Eq. (35) is equivalent to Eq. (6). To do this, we use

$$\sum_{k\geqslant 1}\frac{\varphi_k(\tilde{\boldsymbol{x}}|\boldsymbol{x})\varphi_k^\dagger(\tilde{\boldsymbol{x}}'|\boldsymbol{x})}{\lambda_k} = \frac{1}{\tilde{\gamma}}\int_0^\infty dt[P(\tilde{\boldsymbol{x}}, t|\tilde{\boldsymbol{x}}', 0) - \varphi_0(\tilde{\boldsymbol{x}}|\boldsymbol{x})], \tag{36}$$

where $P(\tilde{\boldsymbol{x}}, t|\tilde{\boldsymbol{x}}', 0) = e^{\tilde{\mathcal{L}}_\mathrm{o}t}\delta(\tilde{\boldsymbol{x}} - \tilde{\boldsymbol{x}}')$ is a propagator starting from $\tilde{\boldsymbol{x}}'$ at time 0 and reaching $\tilde{\boldsymbol{x}}$ at time t. One can verify this relation by using $\varphi_0^\dagger(\tilde{\boldsymbol{x}}|\boldsymbol{x}) = 1$ and $\sum_{k\geqslant 0}\varphi_k(\tilde{\boldsymbol{x}}|\boldsymbol{x})\varphi_k^\dagger(\tilde{\boldsymbol{x}}'|\boldsymbol{x}) = \delta(\tilde{\boldsymbol{x}} - \tilde{\boldsymbol{x}}')$.

By employing the definition of $\boldsymbol{b}_k$ and Eq. (36), we finally arrive at

$$\begin{aligned}\mathsf{G}(\boldsymbol{x}) &= \frac{1}{T}\int_0^\infty dt\Big[\int d\tilde{\boldsymbol{x}}\int d\tilde{\boldsymbol{x}}'\{\nabla_x V_{\rm I}(\boldsymbol{x},\tilde{\boldsymbol{x}})\}\{\nabla_x^{\rm T} V_{\rm I}(\boldsymbol{x},\tilde{\boldsymbol{x}}')\}P(\tilde{\boldsymbol{x}},t|\tilde{\boldsymbol{x}}',0)\varphi_0(\tilde{\boldsymbol{x}}'|\boldsymbol{x}) - \langle\nabla_x V_{\rm I}(\boldsymbol{x},\tilde{\boldsymbol{x}})\rangle_{\rm b}^{\rm eq}\langle\nabla_x^{\rm T} V_{\rm I}(\boldsymbol{x},\tilde{\boldsymbol{x}})\rangle_{\rm b}^{\rm eq}\Big] \\ &= \frac{1}{T}\int_0^\infty dt\Big[\big\langle\{\nabla_x V_{\rm I}(\boldsymbol{x},\tilde{\boldsymbol{x}}(t))\}\{\nabla_x^{\rm T} V_{\rm I}(\boldsymbol{x},\tilde{\boldsymbol{x}}(0))\}\big\rangle_{\rm b}^{\rm eq} - \langle\nabla_x V_{\rm I}(\boldsymbol{x},\tilde{\boldsymbol{x}})\rangle_{\rm b}^{\rm eq}\langle\nabla_x^{\rm T} V_{\rm I}(\boldsymbol{x},\tilde{\boldsymbol{x}})\rangle_{\rm b}^{\rm eq}\Big] \\ &= \frac{1}{T}\int_0^\infty dt\, C_{\nabla_x V_{\rm I},\nabla_x^{\rm T} V_{\rm I}}(t|\boldsymbol{x}),\end{aligned} \tag{37}$$

where $\langle\cdots\rangle_{\rm b}^{\rm eq}$ is an average over the equilibrium bath dynamics for a given $\boldsymbol{x}$.

V. NUMERICAL CONFIRMATION

To verify our analytic results, we performed numerical simulations for two solvable examples with harmonic couplings. The first example is a single particle coupled to a confined bath without translational invariance and the second one is a two-particle system coupled to a bath without mutual independence. In addition, we carried out MD simulations where two-system particles interact with bath particles through a soft elastic repulsion proportional to their overlapped length.

A. Single-particle model without translational invariance

Here, we consider a single-particle system as illustrated in Fig. 3(a). $\tilde{N}$ bath particles ($\tilde{\boldsymbol{x}}$) are confined in a harmonic potential centered at the origin with stiffness $\tilde{k}$ and the system particle (x_1) is coupled to each bath particle via a harmonic potential with stiffness $k_{\rm I}$. Thus, the interaction potential $V_{\rm I} = H_{\rm I} + \tilde{\Phi}$ is given by

$$H_{\rm I}(x_1,\tilde{\boldsymbol{x}}) = \sum_{\tilde{n}}\frac{1}{2}k_{\rm I}(x_1-\tilde{x}_{\tilde{n}})^2, \quad \tilde{\Phi}(\tilde{\boldsymbol{x}}) = \frac{1}{2}\tilde{k}\tilde{\boldsymbol{x}}^{\rm T}\tilde{\boldsymbol{x}}. \tag{38}$$

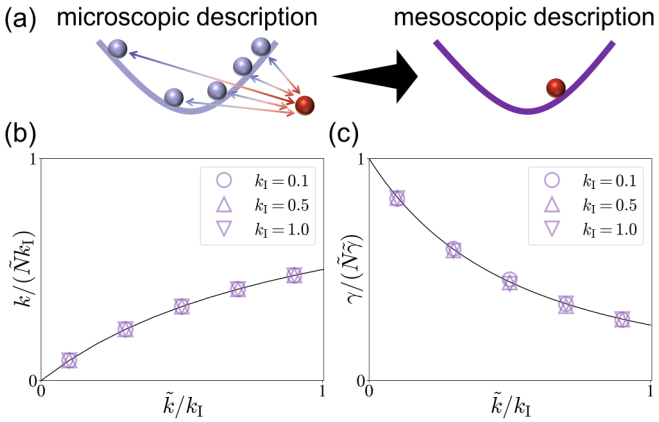

FIG. 3. Simulation results of the single-particle model without translation invariance. (a) Schematic of the model. Interactions between the system and bath particles in the microscopic description can be converted into the effective harmonic potential in the mesoscopic description. (b) Plot for $k/(\tilde{N}k_{\rm I})$ versus $\tilde{k}/k_{\rm I}$ for various $k_{\rm I}$. (c) Plot for $\gamma/(\tilde{N}\tilde{\gamma})$ versus $\tilde{k}/k_{\rm I}$ for various $k_{\rm I}$. The black curves denote the analytical predictions.

The confining potential $\tilde{\Phi}(\tilde{\boldsymbol{x}})$ breaks the translational invariance of $V_{\rm I}$. On the other hand, the mutual independence is satisfied since the system consists of a single particle.

For evaluating the potential of the mean force, it is convenient to rearrange $V_{\rm I}$ as

$$V_{\rm I}(x_1,\tilde{\boldsymbol{x}}) = \sum_{\tilde{n}}\frac{1}{2}(k_{\rm I}+\tilde{k})\tilde{X}_{\tilde{n}}^2 + \frac{\tilde{N}k_{\rm I}\tilde{k}}{2(k_{\rm I}+\tilde{k})}x_1^2, \tag{39}$$

where $\tilde{X}_{\tilde{n}} = \tilde{x}_{\tilde{n}} - k_{\rm I}x_1/(k_{\rm I}+\tilde{k})$. Then, from Eq. (4), the potential of the mean force is

$$\Delta(x_1) = \frac{1}{2}kx_1^2 + \frac{\tilde{N}T}{2}\ln\frac{k_{\rm I}+\tilde{k}}{\tilde{k}}, \tag{40}$$

where $k \equiv \tilde{N}k_{\rm I}\tilde{k}/(k_{\rm I}+\tilde{k})$ is the effective stiffness applied to the system particle. This $\Delta(x_1)$ is tantamount to the harmonic force, $-kx_1$, being exerted on the system particle, which is the consequence of the confinement or broken translational symmetry of the bath particles. It is straightforward to see that the mean force vanishes when the translational symmetry is restored, i.e., $\tilde{k}=0$.

The damping constant (6) is also analytically solvable. Using the Hermitianized Fokker-Plank operator presented in the Supplemental Material [37], the effective damping constant ($\gamma \equiv \mathsf{G}_{1,1}$) can be evaluated as

$$\gamma = \tilde{N}\tilde{\gamma}\left(\frac{k_{\rm I}}{k_{\rm I}+\tilde{k}}\right)^2. \tag{41}$$

Thus, dependence of γ on the interaction strength $k_{\rm I}$ disappears in the limit $\tilde{k}\to 0$ irrespective of the value of $k_{\rm I}$. This is consistent with the analytic prediction (18) that the damping constant becomes independent of interaction potential when the translational invariance is satisfied for a one-particle system.

Equations (40) and (41) indicate that dynamics of the system can be effectively described by the mesoscopic SDE as

$$m\dot{v}_1 = f(x_1,v_1,t) - kx_1 - \gamma v_1 + \sqrt{2\gamma T}\xi_1. \tag{42}$$

Note that the effective damping constant γ vanishes in the weak-interaction limit ($k_I \to 0$), which implies the isolation of the system from the thermal environment. This clearly demonstrates that the conventional Langevin description is not a consequence of the weak interaction.

To confirm our analytic results numerically, we performed a simulation using the microscopic equations of motion (1) with small $\tilde{m}/\tilde{\gamma}$ and small $\tilde{\gamma}$ for proper timescale separation. For simplicity, no external force is applied to the system, i.e., $f(x,v,t)=0$. In this calculation, $\tilde{N}=10^4$, $\tilde{\gamma}=10^{-2}$, $\tilde{m}=10^{-4}$, and $m=T=1$ were used. We evaluated k and γ

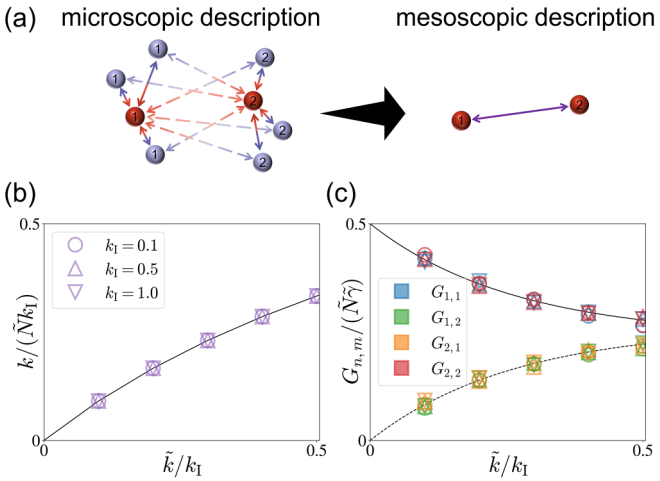

FIG. 4. Simulation results of the two-particle model without mutual independence. (a) Schematic of the model. The solid and dashed arrows indicate the intrainteractions inside the same group and interinteraction between other group particles, respectively. The system-bath interactions in the microscopic description can be converted into the effective harmonic potential in the mesoscopic description. (b) Plot for $k/(\tilde{N}k_I)$ versus κ/k_I for various k_I. The black solid curve denotes the analytical prediction. (c) Plot for $\mathsf{G}_{n,m}/(\tilde{N}\tilde{\gamma})$ versus κ/k_I for various k_I. The black solid and dashed curves denote the analytical predictions for diagonal and off-diagonal elements of G. Circle, up-pointing triangle, and down-pointing triangle represent the numerical data for $k_I = 0.1, 0.5$, and 1.0, respectively. Blue, green, orange, and red colors in (c) represent the data for $\mathsf{G}_{1,1}$, $\mathsf{G}_{1,2}$, $\mathsf{G}_{2,1}$ and $\mathsf{G}_{2,2}$, respectively.

by means of measuring the variance of the position distribution and evaluating the Green-Kubo formula in equilibrium, respectively, for various values of k_I and $\tilde{k}$. To reduce the computational cost, we used the equation of motion for the center of mass coordinate of the bath particles as explained in Supplemental Material [37]. Figures 3(b) and 3(c) are the plots for $k/(\tilde{N}k_I)$ versus $\tilde{k}/k_I$ and $\gamma/(\tilde{N}\tilde{\gamma})$ versus $\tilde{k}/k_I$, respectively. Respective numerical data perfectly fit the analytic formulas of the effective stiffness in Eq. (40) and the effective damping constant (41). This confirms that for a one-particle system the strong coupling effect appears when the translational invariance of the interaction potential is broken.

B. Two-particle model without mutual independence

The second example is a two-particle system interacting with bath particles of two different species as illustrated in Fig. 4(a). In this model, each bath particle is coupled to both system particles via a harmonic potential simultaneously, but with different stiffness depending on its species. In other words, for the nth system particle ($n = 1, 2$) and a bath particle belonging to αth species ($\alpha = 1, 2$), the stiffness $\mathsf{K}_{n,\alpha}$ is given by $\mathsf{K}_{n,\alpha} = k_I$ for $n = \alpha$ and $\mathsf{K}_{n,\alpha} = \kappa$ for $n \neq \alpha$. By setting $\tilde{\Phi} = 0$, the interaction potential $V_I = H_I$ is then written as

$$V_I(\boldsymbol{x}, \tilde{\boldsymbol{x}}) = \frac{1}{2} \sum_{n,\alpha,\tilde{n}_\alpha} \mathsf{K}_{n,\alpha} \left(x_n - \tilde{x}_{\tilde{n}_\alpha}\right)^2. \tag{43}$$

Here, $\tilde{n}_\alpha$ ($1 \leqslant \tilde{n}_\alpha \leqslant \tilde{N}_\alpha$) is the index for a bath particle of the αth species and $\tilde{N}_\alpha$ denotes the number of bath particles belonging to the αth species. Here we consider the case $\tilde{N}_1 = \tilde{N}_2 \equiv \tilde{N}/2$. The nonzero off-diagonal stiffness κ of the K matrix renders the mutual independence broken. Meanwhile, the translational invariance is maintained since all interactions are pairwise.

Similar to the first example, the potential of the mean force can be easily obtained from the rearranged form of the interaction potential as

$$V_I(\boldsymbol{x}, \tilde{\boldsymbol{x}}) = \sum_{\alpha,\tilde{n}_\alpha} \frac{1}{2}(k_I + \tilde{k})\tilde{X}_{\tilde{n}_\alpha}^2 + \frac{\tilde{N}k_I\kappa}{2(k_I + \kappa)}(x_1 - x_2)^2, \tag{44}$$

where $\tilde{X}_{\tilde{n}_\alpha} = x_{\tilde{n}_\alpha} - \sum_n \mathsf{K}_{n,\alpha} x_n/(k_I + \kappa)$. The potential of the mean force is

$$\Delta(\boldsymbol{x}) = \tfrac{1}{2}k(x_1 - x_2)^2 + c, \tag{45}$$

where $k = \tilde{N}k_I\kappa/2(k_I + \kappa)$ and c is a constant without $\boldsymbol{x}$ dependence. Equation (45) indicates that the two-system particles are coupled via an effective harmonic potential with stiffness k, which originates from the harmonic-interaction chain between x_1 and x_2 through the bath particles.

The effective damping tensor is also analytically solvable through the similar technique used for the first example (see Supplemental Material [37]), which is

$$\mathsf{G} = \frac{\tilde{\gamma}\tilde{N}}{2(k_I + \kappa)^2} \begin{pmatrix} k_I^2 + \kappa^2 & 2k_I\kappa \\ 2k_I\kappa & k_I^2 + \kappa^2 \end{pmatrix}. \tag{46}$$

$\Delta(\boldsymbol{x})$ and G are invariant under the permutation of k_I and κ, as this permutation is equivalent to the exchange of the bath species. Thus, we can set $\kappa \leqslant k_I$ without loss of generality. In the limit $\kappa \to 0$, where the mutual independence is restored, k in Eq. (45) vanishes and G in Eq. (46) loses the information on the SB interaction potential and becomes the identity matrix with the overall factor consistent with Eq. (18). In the opposite limit, i.e., $\kappa = k_I$, the effective damping tensor becomes singular because the bath particles are coupled to only one normal mode $x_1 + x_2$.

To check whether the effective dynamics of this two-particle system follows Eq. (5) with Eqs. (45) and (46) numerically, we performed a simulation using the microscopic equations of motion (1). The parameters are set to be the same as in the first example. To ensure the stability of the stationary state, we added an external harmonic force $-k_S\boldsymbol{x}$ with stiffness $k_S = 1.0$ to the system particles.

After the system reaches its equilibrium state, we evaluated the effective stiffness and damping tensor by means of measuring the variance of distance between the two particles and calculating the Green-Kubo formula, respectively. Figures 4(b) and 4(c) show the plots for $k/(\tilde{N}k_I)$ and $\mathsf{G}_{n,m}/(\tilde{N}\tilde{\gamma})$ against κ/k_I for various k_I, respectively. All numerical data coincide with the analytic expectations. This clearly verifies that for a translationally invariant system, the strong coupling effect emerges in the effective dynamics when the mutual independence is broken. It also demonstrates the validity of our formalism in the presence of an external force applied to a system.

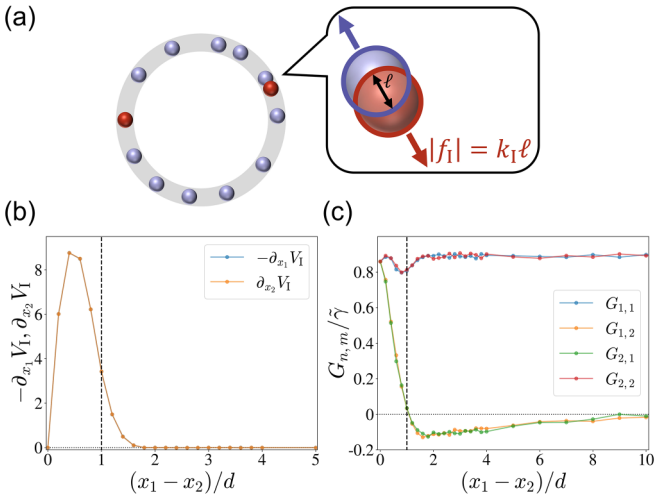

FIG. 5. Results of the MD simulation. (a) Schematic of the two-particle system. Red and blue balls denote system and bath particles, respectively. $\ell = d - |x_n - \tilde{x}_{\tilde{n}}|$ represents the overlapped length between system and bath particles. Arrows indicate the soft repulsion forces whose strength is proportional to ℓ. (b) Plot for mean force versus $(x_1 - x_2)/L$. Blue and orange curves represent the mean force applied to the first particle and minus of the mean force for the second particle, respectively. (c) Plot for $\mathsf{G}_{m,n}/\tilde{\gamma}$ versus $(x_1 - x_2)/L$. Blue, orange, green, and red colors in (c) represent the data for $\mathsf{G}_{1,1}$, $\mathsf{G}_{1,2}$, $\mathsf{G}_{2,1}$ and $\mathsf{G}_{2,2}$, respectively. In both (b) and (c), the vertical dashed line indicates the interaction range $(x_1 - x_2)/d = 1$.

C. Effect of interaction range on mutual independence

Different from the toy models illustrated in Secs. V A and V B, in a usual experimental setup, where multiple particles of the system are immersed together in a single bath, it is almost impossible to satisfy the mutual independence in a strict sense for several reasons. First, a bath particle can move around freely and thus its interacting partner among the system particles may change over time. Therefore, members of a subbath are not fixed in time. Second, a bath particle can interact with several system particles simultaneously when the range of the SB interaction is not sufficiently shorter than the distance between system particles.

In this section, we numerically demonstrate that the mutual independence can be effectively satisfied when the range of SB interaction is much shorter than the distance between system particles, even though the members of subbaths change over time. For this purpose, we performed an MD simulation for a two-particle system moving on a one-dimensional ring with length L, as illustrated in Fig. 5(a). No external force is applied to the two particles and no interaction force exists between them ($\boldsymbol{f} = 0$). There also exist $\tilde{N}$ bath particles moving on the ring that are in contact with the thermostat. Similar to the system particles, no external potential is given to the bath particles, and no interaction force exists between them ($\tilde{\Phi} = 0$). The diameter of the system and bath particles is set to be the same as d. The interaction potential $U(x_n, \tilde{x}_{\tilde{n}})$ between a system particle at x_n and a bath particle at $\tilde{x}_{\tilde{n}}$ is as follows:

$$U(x_n, \tilde{x}_{\tilde{n}}) = \frac{k_I}{2}(|x_n - \tilde{x}_{\tilde{n}}| - d)^2, \tag{47}$$

when the system and bath particles overlap, that is, $|x_n - \tilde{x}_{\tilde{n}}| \leqslant d$. When there is no overlap, $U(x_n, \tilde{x}_{\tilde{n}}) = 0$. The total interaction potential is then given by $V_I(\boldsymbol{x}, \tilde{\boldsymbol{x}}) = \sum_{n,\tilde{n}} U(x_n, \tilde{x}_{\tilde{n}})$. This form of repulsion potential is often employed in various MD simulations [39]. The parameters of this simulation are set as $\tilde{N} = 10^3$, $\tilde{\gamma} = 10^{-2}$, $m = 10^{-2}$, $T = 10$, $k_I = 10$, $d = 1$, and $L = 100$. To reduce the computation time, overdamped Langevin dynamics is assumed for the bath particles, i.e., $\tilde{m} = 0$. After the whole system reaches equilibrium, the mean force can be evaluated using the relation $\nabla_{x_n} \Delta(\boldsymbol{x}) = \langle\{\nabla_{x_n} V_I(\boldsymbol{x}, \tilde{\boldsymbol{x}})\}\rangle_b^{eq}$ from Eq. (4) and the damping tensor $\mathsf{G}_{n,m}$ can be obtained from Eq. (6). Since the translational invariance holds, Δ and G satisfy $\Delta(x_1 + a, x_2 + a) = \Delta(x_1, x_2)$ and $\mathsf{G}(x_1 + a, x_2 + a) = \mathsf{G}(x_1, x_2)$ for any constant a, guaranteeing that they are functions of $x_1 - x_2$ as explained in the Supplemental Material [37].

Figures 5(b) and 5(c) show the dependence of Δ and $\mathsf{G}_{n,m}$ on the relative distance between the system particles $(x_1 - x_2)/d$. In the region $x_1 - x_2 \gg d$, where the range of SB interaction is much shorter than the distance between system particles, Δ and $\mathsf{G}_{n,m}$ exhibit no dependence of $x_1 - x_2$. Especially, off-diagonal elements of $\mathsf{G}_{n,m}$ $(n \neq m)$ vanish in this region. Therefore, the mean force term disappears and G becomes a diagonal and constant matrix, which is consistent with the expectation achieved when mutual independence is satisfied. On the other hand, for $x_1 - x_2 \approx d$, where a bath particle can interact with multiple system particles simultaneously or members of subbaths can change rather quickly, both Δ and G exhibit a certain dependence of $x_1 - x_2$. Therefore, the mean force and off-diagonal elements of G do not vanish, and thus the dynamics relies on the SB interaction.

These observations highlight the dependence of mutual independence's validity on the relative distance between system particles in real-world experiments. If the range of SB interaction is much shorter than the distance between system particles, mutual independence holds effectively. This means that members of subbaths may change over time, but this temporal variation does not significantly affect the validity of their mutual independence. Consequently, under such circumstances, the system's observed dynamics simply follows the conventional Langevin equation, without showing strong coupling effects. On the contrary, if the distance between system particles approaches the scale of SB interaction, the dynamics deviate from the conventional Langevin description. Detecting these SB coupling effects in a multiparticle experiment poses an intriguing and formidable challenge. Since these effects manifest within a restricted spatial domain, densely packing the system particles becomes essential to achieve a distance between them that is comparable to the SB interaction range. Moreover, a measurement apparatus with high spatial resolution is indispensable due to the typically minute scale of SB interaction compared to the system particle size. Without this meticulous experimental preparation, the system's behavior may appear to follow conventional Langevin dynamics, potentially masking the strong coupling effects. In addition, a proper measure applicable to general situations is needed to quantitatively assess whether a multiparticle system satisfies the condition of mutual independence effectively in real experiments or molecular dynamics simulations. Developing such a measure would be an intriguing direction for future work.

VI. DISCUSSION AND PERSPECTIVE

It is instructive to compare our results with those of previous approaches used for deriving the conventional Langevin equation from a microscopic equation of motion. The first such approach uses the kinetic theory based on the Kramers-Moyal expansion introduced to study the Brownian motor [40–42] and adiabatic piston [41,43]. In these models, the system consists of a single degree of freedom, the SB interaction is given by the hard-core collision, and no other potential is applied to bath particles; accordingly, translational invariance and mutual independence are satisfied. Furthermore, the bath particles are assumed to always be in equilibrium, which amounts to an infinitely fast equilibrating thermostat being attached to the bath particles. The microscopic setups of these models are the special case of our general setup satisfying the two conditions described in Sec. III. Therefore, the conventional Langevin equation is derived when the limit of timescale separation is taken into account.

The second approach is the Caldeira-Leggett model [44]. The system of this model also consists of a single particle; thus, mutual independence is satisfied. However, since the SB interaction and the potential applied to the bath particles are not in pairwise forms, the translational invariance is not satisfied. This may lead to a question why the mean force term does not appear in the resulting Langevin equation, even though the translational invariance of the potential is broken. This is due to the counterterm conventionally added to the total Hamiltonian of the Caldeira-Leggett model. In the derivation of the Langevin equation, the mean-force-like term is eventually canceled out by the counterterm. We also note that this approach does not take any explicit timescale separation methods. Instead, the special form of interactions and spectral functions are assumed, which make the system dynamics Markovian.

The third one considers Hamiltonian dynamics, where a heavy particle is immersed in an environment consisting of lighter bath particles [29]. In the limit of small mass for the bath particles, relevant studies have demonstrated that the dynamics of the heavy particle can be described by the conventional Langevin equation [29–33]. The primary distinction between this approach and ours lies in the treatment of bath dynamics. While the former models the dynamics of the entire system-bath using a deterministic Hamiltonian, our work considers stochastic evolution of the bath particles' motions under the influence of the super bath. Therefore, in our formalism, no additional conditions besides timescale separation are necessary to maintain the equilibrium state of the bath, whereas Hamiltonian dynamics require further assumptions. Moreover, previous studies have focused on the motion of single-particle systems and pairwise interactions, naturally leading to the conventional Langevin equation. However, our paper aims to uncover the effects of arbitrary SB interactions and determine the conditions under which these effects disappear.

More recently, the conventional Langevin equation has also been derived for systems in which a tracer particle interacts with a fluctuating field [45–47]. Our study differs from these works primarily in how we describe bath dynamics. While the mentioned works utilize a coarse-grained fluctuating field, our approach relies on an explicit equation of motion for the bath particles.

We anticipate that our formalism will open the way to investigate thermodynamics for stochastic systems strongly coupled to baths and be utilized to simulate such systems without directly performing an MD simulation, so as to reduce the computational cost significantly.

ACKNOWLEDGMENTS

The authors acknowledge the Korea Institute for Advanced Study for providing computing resources (KIAS Center for Advanced Computation Linux Cluster System). This research was supported by NRF Grant No. 2017R1D1A1B06035497 (H.P.), and individual KIAS Grants No. QP013601 (H.P.), No. PG064902 (J.S.L.), and No. PG074002 (J.-M.P.) at the Korea Institute for Advanced Study. This research was supported by an appointment to the JRG Program at the APCTP through the Science and Technology Promotion Fund and Lottery Fund of the Korean Government (J.-M.P.). This was also supported by the Korean Local Governments—Gyeongsangbuk-do Province and Pohang City (J.-M.P.).

[1] C. Jarzynski, Nonequilibrium equality for free energy differences, Phys. Rev. Lett. **78**, 2690 (1997).

[2] G. E. Crooks, Entropy production fluctuation theorem and the nonequilibrium work relation for free energy differences, Phys. Rev. E **60**, 2721 (1999).

[3] J. Kurchan, Fluctuation theorem for stochastic dynamics, J. Phys. A: Math. Gen. **31**, 3719 (1998).

[4] U. Seifert, Entropy production along a stochastic trajectory and an integral fluctuation theorem, Phys. Rev. Lett. **95**, 040602 (2005).

[5] A. C. Barato and U. Seifert, Thermodynamic uncertainty relation for biomolecular processes, Phys. Rev. Lett. **114**, 158101 (2015).

[6] T. R. Gingrich, J. M. Horowitz, N. Perunov, and J. L. England, Dissipation bounds all steady-state current fluctuations, Phys. Rev. Lett. **116**, 120601 (2016).

[7] T. R. Gingrich, G. M. Rotskoff, and J. M. Horowitz, Inferring dissipation form current fluctuations, J. Phys. A: Math. Theor. **50**, 184004 (2017).

[8] P. Pietzonka, F. Ritort, and U. Seifert, Finite-time generalization of the thermodynamics uncertainty relation, Phys. Rev. E **96**, 012101 (2017).

[9] J. M. Horowitz and T. R. Gingrich, Proof of the finite-time thermodynamics uncertainty relation for steady-state currents, Phys. Rev. E **96**, 020103(R) (2017).

[10] A. Dechant, Multidimensional thermodynamic uncertainty relations, J. Phys. A: Math. Theor. **52**, 035001 (2019).

[11] Y. Hasegawa and T. V. Vu, Uncertainty relation in stochastic processes: An information inequality approach, Phys. Rev. E **99**, 062126 (2019).

[12] T. V. Vu and Y. Hasegawa, Uncertainty relations for underdamped langevin dynamics, Phys. Rev. E **100**, 042907 (2019).

[13] J. S. Lee, J.-M. Park, and H. Park, Thermodynamic uncertainty relation for underdamped langevin systems driven by a velocity-dependent force, Phys. Rev. E **100**, 062132 (2019).
[14] N. Shiraishi, K. Funo, and K. Saito, Speed limit for classical stochastic processes, Phys. Rev. Lett. **121**, 070601 (2018).
[15] V. T. Vo, T. Van Vu, and Y. Hasegawa, Unified approach to classical speed limit and thermodynamic uncertainty relation, Phys. Rev. E **102**, 062132 (2020).
[16] T. Van Vu and Y. Hasegawa, Geometrical bounds of the irreversibility in Markovian systems, Phys. Rev. Lett. **126**, 010601 (2021).
[17] K. Yoshimura and S. Ito, Thermodynamic uncertainty relation and thermodynamic speed limit in deterministic chemical reaction networks, Phys. Rev. Lett. **127**, 160601 (2021).
[18] S. Ito and A. Dechant, Stochastic time evolution, information geometry, and the Cramér-Rao bound, Phys. Rev. X **10**, 021056 (2020).
[19] G. Falasco and M. Esposito, Dissipation-time uncertainty relation, Phys. Rev. Lett. **125**, 120604 (2020).
[20] S. B. Nicholson, L. P. García-Pintos, A. del Campo, and J. R. Green, Time–information uncertainty relations in thermodynamics, Nat. Phys. **16**, 1211 (2020).
[21] F. Tasnim and D. H. Wolpert, Thermodynamic speed limits for co-evolving systems, arXiv:2107.12471.
[22] A. Dechant, Minimum entropy production, detailed balance and Wasserstein distance for continuous-time Markov processes, J. Phys. A: Math. Theor. **55**, 094001 (2022).
[23] J.-C. Delvenne and G. Falasco, Thermokinetic relations, Phys. Rev. E **109**, 014109 (2024).
[24] J. S. Lee, S. Lee, H. Kwon, and H. Park, Speed limit for a highly irreversible process and tight finite-time Landauer's bound, Phys. Rev. Lett. **129**, 120603 (2022).
[25] C. Kwon, J. Um, J. Yeo, and H. Park, Three heats in a strongly coupled system and bath, Phys. Rev. E **100**, 052127 (2019).
[26] P. Strasberg and M. Esposito, Stochastic thermodynamics in the strong coupling regime: An unambiguous approach based on coarse graining, Phys. Rev. E **95**, 062101 (2017).
[27] U. Seifert, First and second law of thermodynamics at strong coupling, Phys. Rev. Lett. **116**, 020601 (2016).
[28] C. Jarzynski, Stochastic and macroscopic thermodynamics of strongly coupled systems, Phys. Rev. X **7**, 011008 (2017).
[29] P. Mazur and I. Oppenheim, Molecular theory of Brownian motion, Physica **50**, 241 (1970).
[30] J. L. Lebowitz and E. Rubin, Dynamical study of Brownian motion, Phys. Rev. **131**, 2381 (1963).
[31] P. Resibois and H. T. Davis, Transport equation of a Brownian particle in an external field, Physica **30**, 1077 (1964).
[32] J. L. Lebowitz and P. Resibois, Microscopic theory of Brownian motion in an oscillating field; connection with macroscopic theory, Phys. Rev. **139**, A1101 (1965).
[33] H. Mori, Transport, collective motion, and Brownian motion, Prog. Theor. Phys. **33**, 423 (1965).
[34] P. Talkner and P. Hänggi, Colloquium: Statistical mechanics and thermodynamics at strong coupling: Quantum and classical, Rev. Mod. Phys. **92**, 041002 (2020).
[35] L. Van Hove, The approach to equilibrium in quantum statistics: A perturbation treatment to general order, Physica **23**, 441 (1957).
[36] H. Risken, *The Fokker-Planck Equation, Methods of Solution and Applications* (Springer, Berlin, Heidelberg, 1996).
[37] See Supplemental Material at http://link.aps.org/supplemental/10.1103/PhysRevE.110.014143 for detailed explanations of the pairwise property of translational invariant functions, generalized Green-Kubo relation, the derivation of the damping coefficients in the first and second examples, and the equation of motion for the center of mass coordinates, which includes Ref. [38].
[38] G. A. Pavliotis, *Stochastic Processes and Applications* (Springer, New York, NY, 2015).
[39] M. Han, M. Fruchart, C. Scheibner, S. Vaikuntanathan, J. J. De Pablo, and V. Vitelli, Fluctuating hydrodynamics of chiral active fluids, Nat. Phys. **17**, 1260 (2021).
[40] C. Van den Broeck, R. Kawai, and P. Meurs, Microscopic analysis of a thermal Brownian motor, Phys. Rev. Lett. **93**, 090601 (2004).
[41] P. Meurs, C. Van den Broeck, and A. Garcia, Rectification of thermal fluctuations in ideal gases, Phys. Rev. E **70**, 051109 (2004).
[42] J. S. Lee, J.-M. Park, J. D. Noh, and H. Park, Geometry-induced rectification for an active object, Phys. Rev. Res. **3**, L042011 (2021).
[43] J. Piasecki and C. Gruber, From the adiabatic piston to macroscopic motion induced by fluctuations, Physica A **265**, 463 (1999).
[44] A. O. Caldeira and A. J. Leggett, Path integral approach to quantum Brownian motion, Physica A **121**, 587 (1983).
[45] V. Démery and D. S. Dean, Perturbative path-integral study of active-and passive-tracer diffusion in fluctuating fields, Phys. Rev. E **84**, 011148 (2011).
[46] V. Démery, Diffusion of a particle quadratically coupled to a thermally fluctuating field, Phys. Rev. E **87**, 052105 (2013).
[47] D. Venturelli, F. Ferraro, and A. Gambassi, Nonequilibrium relaxation of a trapped particle in a near-critical Gaussian field, Phys. Rev. E **105**, 054125 (2022).